Arch. Metall. Mater. **64** (2019), 1, 243-250

DOI: 10.24425/amm.2019.126244

P. SAWICKA-CHUDY*[#], G. WISZ**, M. SIBIŃSKI***, M. CHOLEWA*, P. POTERA**, Ł. GŁOWA****, R. PAWEŁEK*****

OPTICAL AND STRUCTURAL PROPERTIES OF Cu_2O THIN FILM AS ACTIVE LAYER IN SOLAR CELLS PREPARED BY DC REACTIVE MAGNETRON SPUTTERING

A series of copper oxide thin films were synthesized through direct current magnetron sputtering on glass and silicon substrates with various process parameters. Initially, optical microscopy images and their histograms were analyzed to determine the optical quality of the obtained layers and then histograms were created using Image Histogram Generator software. Next, the morphology, and cross-section and layer composition of the samples were evaluated. Finally, the transmission spectra of the thin films were recorded. Transmittance and reflection spectra of the UV–vis analysis were utilized to calculate the optical band gap, the extinction coefficient, and the absorption coefficient of the oxidized layers. Samples showed low transmittance (up to 40%) in the region of 400 to 1000 nm. The mean absorption coefficient varied from ~$3 \cdot 10^5$ to ~$6 \cdot 10^5$ 1/cm and from ~$2 \cdot 10^5$ to ~$4 \cdot 10^5$ 1/cm in the region of 2 eV to 3.5 eV. The extinction coefficient ranged from 0 to 0.11 in the region from 300 to 3000 nm. Reflectance of the samples was ~20% in the region of 1000 to 2500 nm and ranged from 20%-50% in the region of 1000 to 3000 nm. We verified the process parameters of the Cu_2O structure to improve the quality as a buffer layer. On the basis of this preliminary analysis, we propose the most promising and future-oriented solutions in photovoltaic applications.

Keywords: Cu_2O thin films, Optical properties, Surface properties, Compositional properties, Energy band gap

1. Introduction

Cuprous oxide (Cu_2O) and cupric oxide (CuO) are p-type semiconductors [1] with band gaps of 2.0-2.6 eV and 1.21-1.51 eV, respectively [1,2]. Many techniques are used to deposit Cu_2O thin films. Researchers obtained copper oxide thin films by spray pyrolysis technique (SPT) [3], spin coating [4], dip coating [5], successive ionic layer adsorption and reaction SILAR [6], physical vapour deposition [7], chemical vapor deposition [8], pulsed laser deposition [9], sol-gel [10], plasma based ion implantation and deposition [11], solution growth [12], molecular beam epitaxy [13] and magnetron sputtering [14]. Reactive direct current (DC) magnetron sputtering is one of the best techniques because it allows for good control of the chemical composition and a high deposition rate at low substrate temperatures [15,16]. The physical properties of the copper oxide films obtained using the magnetron sputtering technique are influenced by the process parameters, such as oxygen partial pressure, substrate temperature, sputtering power, and sputtering pressure [15]. Copper oxide has numerous advantages, such as low production cost, non-toxic nature, abundant availability [15], simple preparation process among oxides, and an individual square planar coordination of copper by oxygen [1]. Thus, copper oxide thin films are available in many applications such as heterojunction solar cells, electrochromic devices, oxygen and humidity sensors [15], optical switches, field emitters, electrode materials for lithium batteries, magneto-resistive materials, catalysts, high temperature superconductors, soil lignin study, a cathode in lithium primary cells, effect transistors [1,17-19].

Properties of substrate made of copper oxides of thin films prepared by reactive DC magnetron sputtering was subject of experimental work of many other authors. Zhu et al. investigated the influences of oxygen partial pressure and gas flow rate on the structures and properties thin films [15]. Kamimura et al. found the substrate temperature and oxygen partial pressure are important parameters in controlling the film property [20]. Reddy et al. studied the influence of oxygen partial pressure on the structural and optical properties of Cu_2O films [21]. Reddy et al. found the crystalline orientation mainly depends on the sputtering pressure [22]. Reddy et al. investigated structural, composition, microstructure, surface morphology, optical and electrical properties Cu_2O thin films and proposed to prepare thin film for optoelectronic devices [23].

Metal-semiconductors are used in heterojunction solar cells fabricated using Cu_2O as the active layer. The conversion efficiency is the most important property in photovoltaic

* UNIVERSITY OF RZESZOW, FACULTY OF MATHEMATICS AND NATURAL SCIENCES, DEPARTMENT OF BIOPHYSICS, 1 PIGONIA STR., 35-317 RZESZOW, POLAND
** UNIVERSITY OF RZESZOW FACULTY OF MATHEMATICS AND NATURAL SCIENCES, DEPARTMENT OF EXPERIMENTAL PHYSICS, 1 PIGONIA STR., 35-317 RZESZOW, POLAND
*** ECOEFFECT SP. Z O.O. [LTD.], KARDYNAŁA STEFANA WYSZYŃSKIEGO 6B/6, 39-300 MIELEC, POLAND
**** LODZ UNIVERSITY OF TECHNOLOGY, DEPARTMENT OF SEMICONDUCTOR AND OPTOELECTRONIC DEVICES, WÓLCZAŃSKA 211/215 STREET, 90-924 LODZ, POLAND
***** LODZ UNIVERSITY OF TECHNOLOGY, INSTITUTE OF ELECTRICAL POWER ENGINEERING, STEFANOWSKIEGO 18/22 STREET, 90-924 LODZ, POLAND

[#] Corresponding author: psawicka@ur.edu.pl

TABLE 1

Photovoltaic characteristics of solar cells fabricated using Cu_2O as the active layer [27-34] where: η is efficiency of solar cell, Voc is open circuit voltage, Jsc is short-circuit current density, and FF is fill facto

Solar cell	Photovoltaic characteristics	Source
ZnO (ZO)/Cu_2O	η = 3.83%, Voc = 0.69 V, FF= 0.55	T. Minami et al. (2011) [27]
Cu–Cu_2O	η = 1.76%, Jsc = 12-14 mA/cm^2	L. C Olsen et al. (1982) [28]
TCO/Cu_2O	Voc = 0.595 V, Jsc = 6.78 mA/cm^2, FF = 0.5, η = 2%	Mittiga et al. (2006) [29]
Cu_2O/ZnO	η = 0.40%, Voc = 0.26 V, Jsc = 2.8 mA/cm^2, FF = 0.55	K. Akimoto et al. (2006) [30]
TiO_2/Cu_2O	η = 0.15%,	S. Hussain et al. (2012) [31]
TiO_2/Cu_2O	η = ~0.01%, Jsc = 0.33 mA/cm^2, Voc = 0.1 V, FF = 0.27	D. Li et al. (2011) [32]
TiO_2/Cu_2O	η = 0.0005%, Jsc = 0.0031 mA/cm^2, Voc = 0.47 V,	A.R. Zainun et al. (2012) [33]
TiO_2/CuO	η = 0.14%,Voc = 0.62 V, Jsc = 0.08 mA/cm^2, FF = 0.33	M. Rokhmat et al. (2017) [34]
TiO_2/CuO/Cu	η = 1.62%,Voc = 0.64 V, Jsc = 0.72 mA/cm^2, FF = 0.42	M. Rokhmat et al. (2017) [34]

(PV) devices [24]. Although the theoretical limit of the energy conversion efficiency of a Cu_2O solar cell is ~20% [25,26], the highest efficiency obtained on Cu_2O substrates is much lower. Table 1 shows the PV characteristics of solar cells published in the literature.

Minami et al. created low-cost n-p heterojunction oxide solar cells with an Al-doped ZnO (AZO)/non-doped ZnO (ZO)/ Cu_2O structure [27]. Olsen et al. produced cells through the oxidation of high-purity copper disks with p-type resistivities of about 10-100 ohm-cm by providing a low partial pressure of chlorine during oxidation [28]. Mittiga et al. reported the fabrication of heterojunction solar cells by depositing transparent conducting oxide (TCO) films on Cu_2O substrates [29]. Akimoto et al. studied polycrystalline p-Cu_2O/n-ZnO heterojunctions grown by radio-frequency magnetron sputtering [30]. Hussain et al. fabricated p-Cu_2O/n-TiO_2 thin-film heterojunction solar cells by electrodeposition of Cu_2O on radio-frequency–sputtered n-TiO_2 thin films [31]. Li et al. fabricated and tested 10 devices with Cu_2O/TiO_2. Solar cells exhibited improved PV characteristics after the post-annealing process (200°C for 1 h under Ar flow with an active area of 0.057 cm^2) [32]. Cu_2O films were deposited by electrochemical deposition on TiO_2 films prepared by the squeegee method, and a cell was generated by evaporating In on the film. Zainun et al. used the squeegee method for electrochemical deposition of Cu_2O on TiO_2 films, and a cell was generated by evaporating In on the film [33]. Rokhmat et al. measured and compared the performance of TiO_2/CuO solar cells before (denoted by TiO_2/CuO solar cells) and after insertion of the copper particles using fixed-current electroplating with a current source of 1.0 mA for 10 s (denoted as TiO_2/CuO/Cu) [34]. The best results are shown in Table 1.

Copper oxide films were prepared by reactive DC magnetron sputtering, which allows for high deposition rates and different substrate temperatures. Cuprous oxide can be used as an active layer in PV devices based on semiconductor oxides [35]. Cu_2O thin films act as active layers in photovoltaic structures because of their high absorption and function as a semiconductor with a low band-gap value. Proper band-gap, structural, optical, and thermal properties are suitable for heterojunction construction with a buffer layer. Cu_2O(CuO) thin films can also be prepared by various other techniques. Technologic modifications are aimed at improving copper oxides for use as active layers in PV devices for potential applications in semiconductor solar cells.

2. Experimental

Commercial N-type Si (100) wafers and plain glass slides, 5×4 and 6×5 mm, respectively, were used as the substrate materials. Several Cu_2O structures were deposited by DC magnetron sputtering using a metal Cu target (purity N 99.995, diameter of 253 mm) under an Ar (99.99%) and O_2 (99.99%) mixed atmosphere with different process parameters selected on the basis of earlier studies and numerical simulations [14, 26, 36,37]. Pressure gauges were used to control the pressure during the sputtering procedure. The sputtering time was strictly adjusted to 40 min and 60 min. The methods were tested and compared to observe their influence on the optical parameters, morphology, composition, and structure of the thin films. We present representative layers from a series of studies. The process parameters are shown in Table 2.

TABLE 2

Process parameters

Parameter	P1 Sample	P2 Sample
Date of manufacture	B1	B2
Method used for preparation	DC reactive sputtering	
Thickness of layer [nm]	~2500	~1000
Distance between the source and substrate [mm]	38	58
Pressure process [mbar]	$1.73 \cdot 10^{-2}$	$2.5 \cdot 10^{-2}$
Power [W]	~80	~70
Time [min]	40	60
Oxygen flow rates [cm^3/s]	3	8
Argon flow rates [cm^3/s]	2	2
Substrate temperature [K]	473.15	473.15

Initially, basic material properties such as thickness and optical properties were examined. Thicknesses were studied using a ContourGT profilometer and then optical microscope images

were recorded using a Nikon Eclipse MA200 at a magnification of 500x. Next, the composition and morphology of the films were investigated with a scanning electron microscope (Tescan Vega3), which was equipped with an energy dispersive X-ray spectroscopy analyzer. Finally, the transmissions spectra of the thin films were recorded using a CARY 5000 spectrophotometer.

3. Results

3.1. Images from optical microscope

Figure 1 shows the optical microscopy images on a glass sample at a magnification of 500× and their histograms. To determine the optical quality of the obtained layers, images were obtained using an optical microscope. The optical quality is related to the morphology and opto-electronic characteristics of the thin films, which may be confirmed by SEM analysis and optical measurements. The histograms were created using Image Histogram Generator software, which is available online [38]. As can be observed in Figure 1, the thin films were not homogeneous and there were many different size defects. Some of them formed an elongated shape, while others were irregular with sizes up to ~0.2 μm. Using the data obtained with Image Histogram Generator software, we calculated the standard deviation, which is presented in Table 3.

TABLE 3

Calculated standard deviation

Sample	Standard deviation	Mean (pixel)
P1	15	135
P2	10	122

Table 2 shows that the P2 samples had the lowest standard deviation, and thus it is expected that they would have the best optical quality.

3.2. Morphological properties

The morphology of nanomaterials markedly affects their physical and chemical properties. Thus, basic studies to evaluate morphology are important. Figure 2 shows SEM images of Cu_2O thin films deposited on silicon substrates at 30 kV. The images were obtained at this voltage because it provided the best resolution. The SEM images were obtained for the area with the least number of defects. Only the P1 samples were uniform. The P2 samples were smooth, but there were many different-sized defects. The optical quality of the obtained layers is related to their morphology and opto-electronic qualities, which may be confirmed by SEM analysis and optical measurements. We studied the full set of obtained samples.

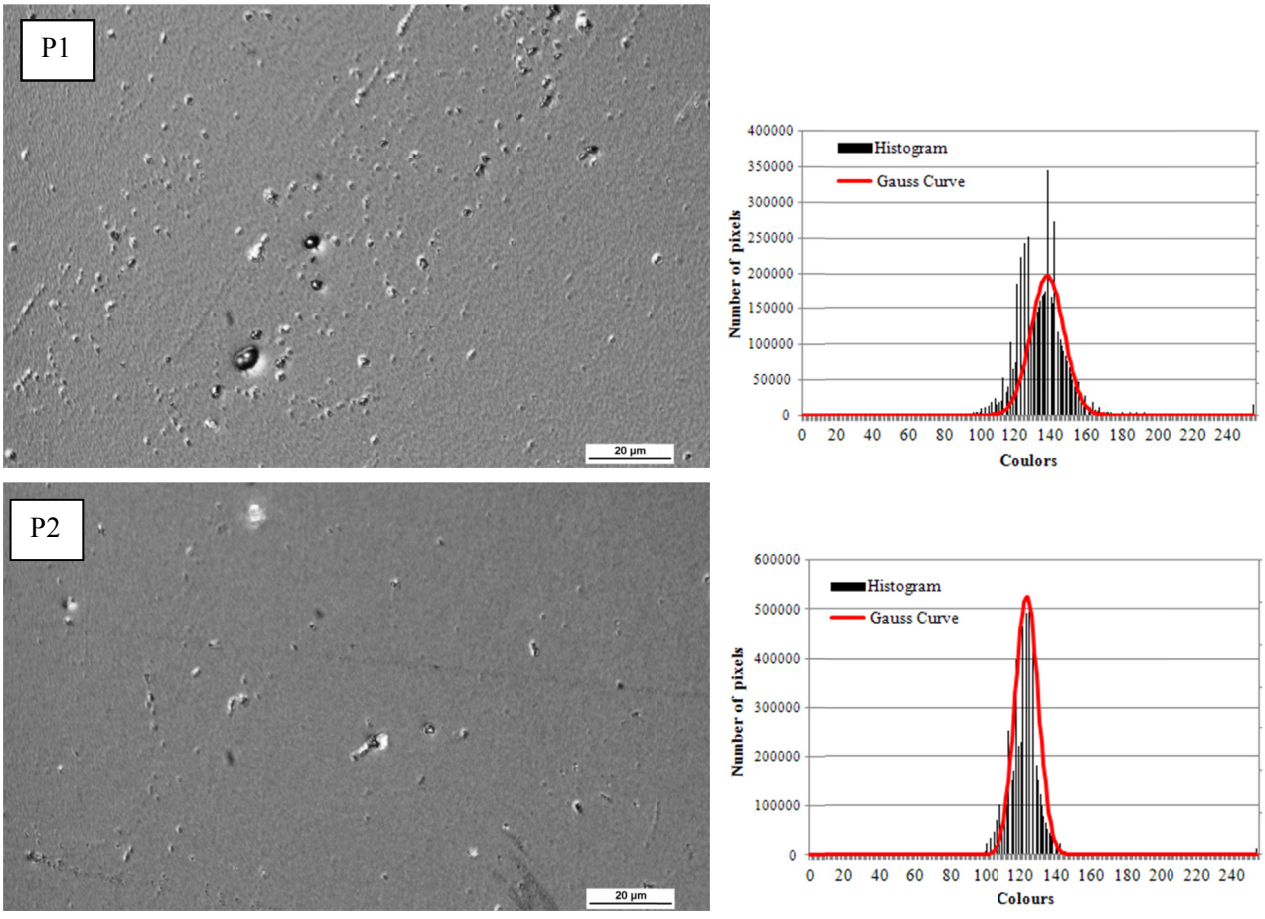

Fig. 1. Optical microscopy images and their histograms

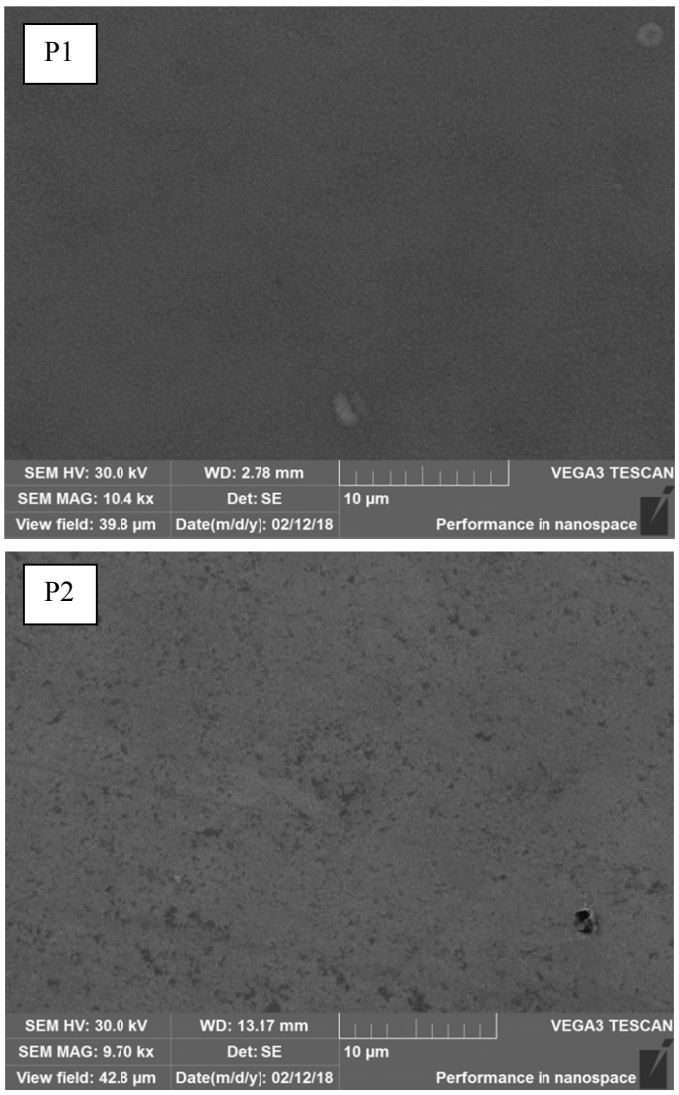

Fig. 2. SEM images of pure Cu_2O thin films deposited on silicon substrates

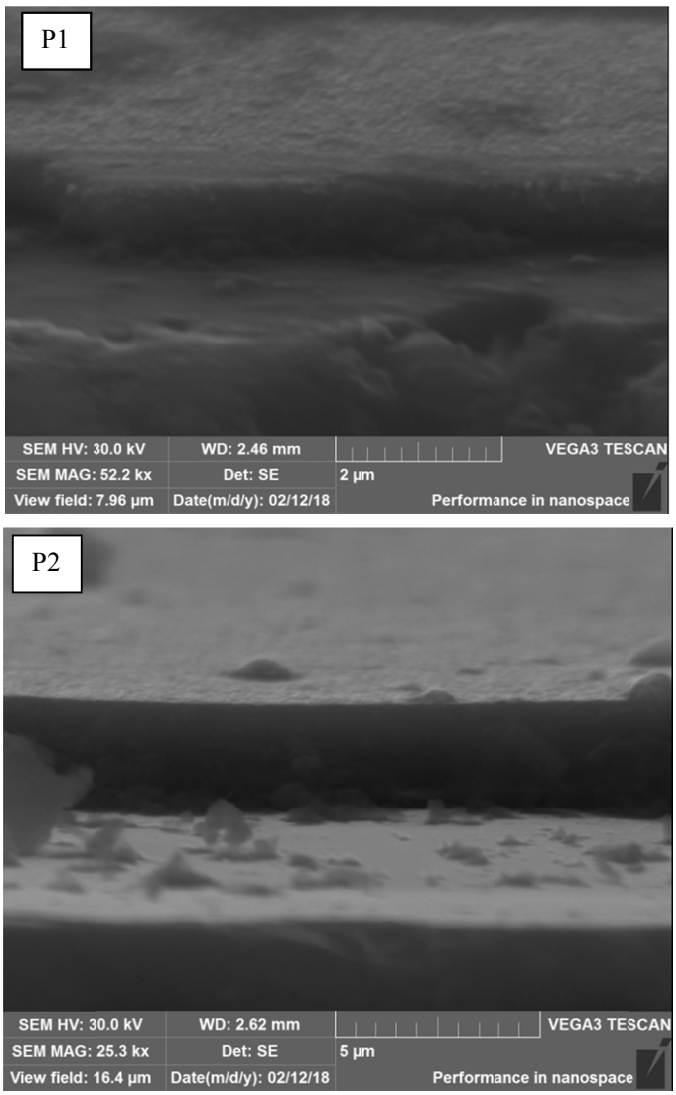

Fig. 3. Cross-section of TiO_2 thin films deposited on silicon substrates

Fig. 3 shows a cross section of Cu_2O thin films in various scales. The cross-section of P1 and P2 appeared smooth and homogeneous with a columnar-type growth. The columnar surface effectively increases the contact area between the active layer and buffer layer, and allows for more efficient hole injection and thus improved PV devices [39].

TABLE 4

Particular composition at the atomic percent

	P1 [%]	**P2 [%]**
Oxygen	37	39
Copper	63	61
Cu:O (ratio)	1.70	1.56

3.3. Composition

Energy dispersive x-ray spectroscopy (EDS) was performed to determine the Cu and O content of the films. Measurements of layers were obtained at a low accelerating voltage (5 kV) due to the small thickness of the films on a silicon substrate. Table 4 shows the atomic percent compositions of the thin films calculated without silicon.

The EDS study revealed that the films did not have similar compositions. While it was assumed that no free oxygen would be present in any of the samples, excess oxygen was observed with respect to copper. The analysis revealed that P1 thin films possessed a near perfect Cu_2O stoichiometry and P2 films possessed a near perfect Cu_2O_3 stoichiometry. In P1 sample, there were some defects in the structure that could lead to different Cu:O ratios. Mencer et al. presented experimental work on Cu_3O_2 in the early 1960s [40].

3.4. Optical properties

Transmittance of the film was determined for wavelengths ranging from 350 to 3000 nm. The effects of thickness on the optical transmittance (T) and the band gap (E_g) values of the

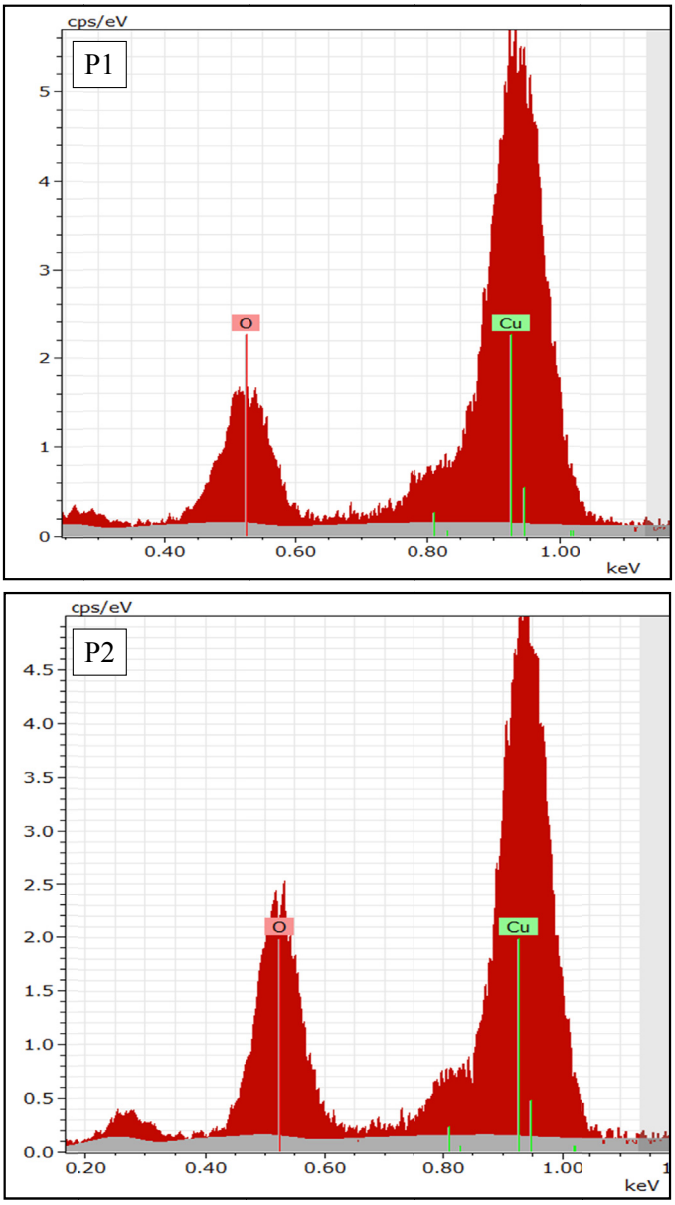

Fig. 4. Composition measured at 5 kV

Cu_2O films were studied. The optical transmission spectra of the Cu_2O films (P1, P2) are shown in Fig. 5.

The average optical transparency films increased from ~10% to 40% in the region of 400 to 1300 nm, which is due to the increase in the sputtering pressure from $1.73 \cdot 10^{-2}$ to $2.5 \cdot 10^{-2}$ mbar. At low sputtering pressures, the defect centers present in the films scattered the light and decreased the transmittance values. By increasing the sputtering pressure, the defect center density decreased, resulting in an increase in the transmittance value [22]. Reddy et al. [22] and Meng et al. [41] noticed similar behavior in Cu_2O films and in ZnO films, respectively, produced by DC magnetron sputtering.

Figure 6 shows the transmittance of Cu_2O films as a function of light quantum energy. The P1 sample passed from 0% to ~20%, and the P2 sample passed from 0% to 40%, as the photon energy between 0.5 and 2.0 eV corresponds at 619-2478 nm. For P1 and P2, the transmittance decreased continuously between

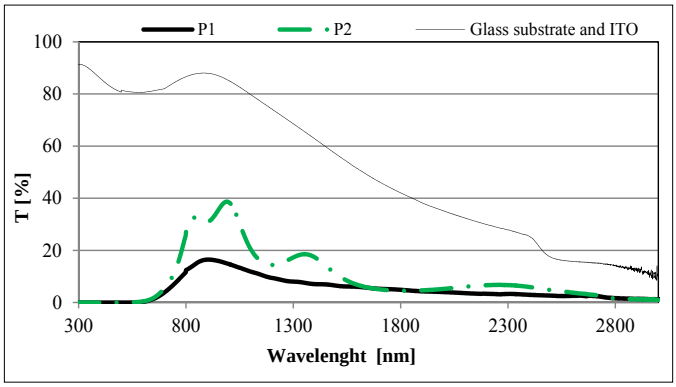

Fig. 5. Optical transmission spectra of the samples (P1, P2) on thin film Cu_2O

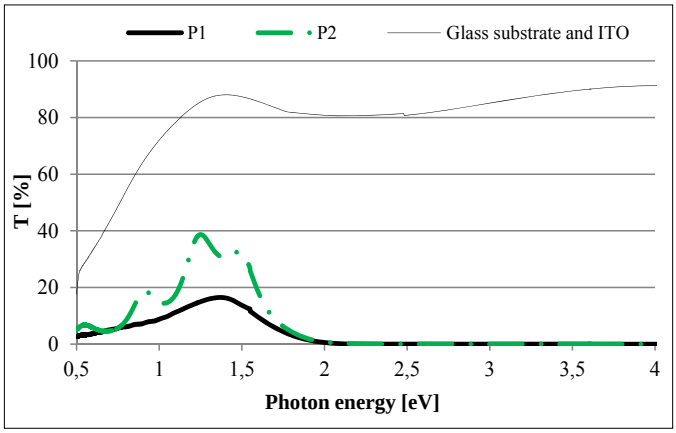

Fig. 6. Transmittance of the thin film Cu_2O (P1, P2, P3)

1.4 and 2.0 eV, and 1.5 and 2 eV, respectively. This is because of the onset of fundamental absorption [42].

From the measured transmittance, the authors calculated the absorption coefficient α using the following relation [25]:

$$\alpha \approx \frac{1}{d} \ln\left(\frac{1}{T}\right) \tag{1}$$

where d is the thickness of the film (Table 1) and T is its transmittance region. Fig. 7 shows absorption versus photon energy (hv).

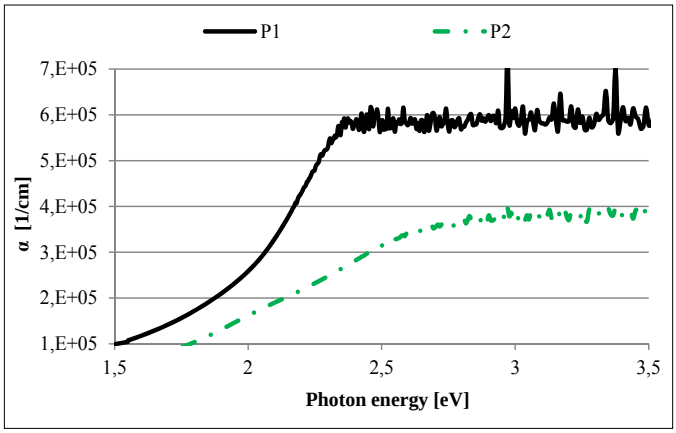

Fig. 7. Absorption coefficient for P1, P2 and P3

The absorption coefficient invariably shows a non-zero value for energies well below the gap [43]. As shown in Figure 7, the mean absorption coefficient for the P1 and P2 samples ranged from ~$3 \cdot 10^5$ to ~$6 \cdot 10^5$ 1/cm and from ~$2 \cdot 10^5$ to ~$4 \cdot 10^5$ 1/cm in the region of 2 eV to 3.5 eV, respectively. They are in fairly good agreement with the literature data obtained from Ito et al. [43,44] in the energy range from 2.1 to 2.4 eV.

Extinction coefficients of the layers (k) were calculated by using transmittance spectra and the equation [25]:

$$k = \frac{\alpha\lambda}{4\pi} \tag{2}$$

Fig. 8 shows the extinction coefficient k for P1, P2.

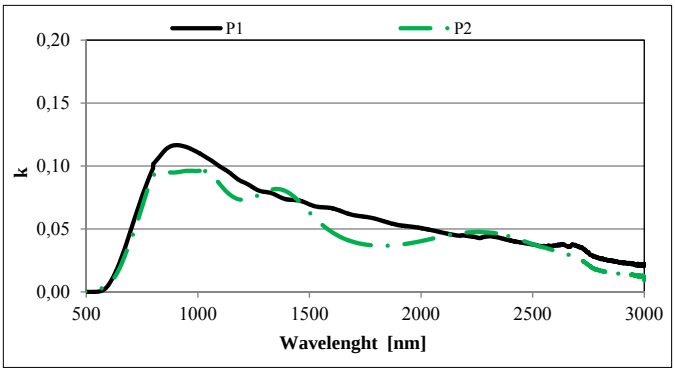

Fig. 8. Extinction coefficient (k) for P1, P2 and P3

The low value of the extinction coefficient (<0.01) is a qualitative indication of the excellent surface smoothness of the prepared samples [45]. For P1 and P2, the extinction coefficient increased to ~1000 nm and then decreased. The optical quality of all thin films is relatively high. This is evident by the low extinction coefficient values (between 0 and 0.11) in the region from 500 to 3000 nm.

For the direct transition, the optical band gap energy of films was determined using the equation [46]:

$$\alpha h\nu = A(h\nu - E_g)^m \tag{3}$$

where α is absorbance, $h\nu$ is photon energy, E_g is the optical band gap, A is denoted as the band tailing parameter. The value of m should be taken as 1/2, according to theoretical and experimental results for direct transition in Cu_2O [47]. To calculate the direct band gap, $(\alpha h\nu)^2$ is plotted as a function of photon energy $E = h\nu$, shown in Fig. 9.

Figure 9 shows that the optical band gap values of the P1 and P2 samples shifted slightly toward copper (II) oxide. The optical band gap obtained in the present investigation is in good agreement with that reported by Reddy et al. [21]. DC reactive magnetron-sputtered Cu_2O films showed an optical band gap of 2.04 eV at $2 \cdot 10^{-2}$ Pa.

The mean reflectance for the P1 sample was ~20% in the region of 1000 to 2500 nm and 20% to ~50% for the P2 sample, in the region of 1000 to 3000 nm. The different properties were due to differences in light scattering resulting from the various

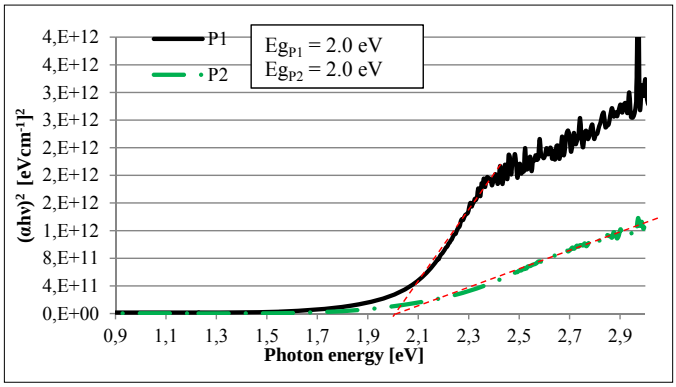

Fig. 9. Optical absorption coefficients α of samples (P1, P2, P3) as a function of incident photon energy by indirectly allowed transitions

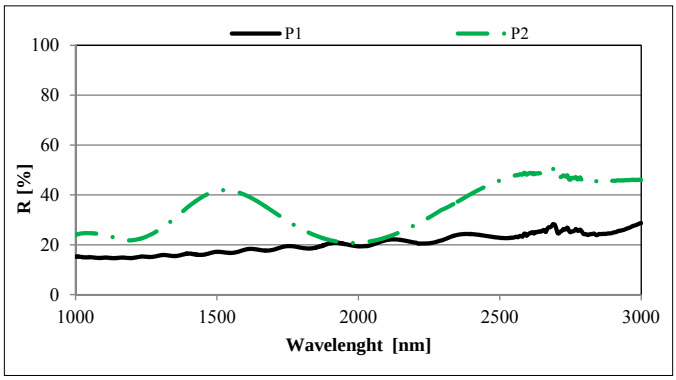

Fig. 10. Reflection spectra of the thin film Cu_2O (P1, P2)

crystal dimensions effect [48]. The mean reflectance of the films increased with an increase in the sputtering pressure from $1.73 \cdot 10^{-2}$ to $2.5 \cdot 10^{-2}$ mbar. Reddy et al. [22] also observed that the refractive index of the films increased with an increase in the sputtering pressure.

4. Conclusions

Cu_2O thin films were deposited by direct current magnetron sputtering on commercially available indium tin oxide-coated glass square and silicon substrates at 473.15 K from a Cu target. Technological modifications were aimed at improving the copper oxides as active layers for PV devices.

The main conclusions were as follows:

- The optical microscopy images and SEM images show that the films were not smooth and there were many different sized point defects. The P2 sample had better optical quality based on analysis of the optical histograms.
- The P1 and P2 thin films tended to exhibit columnar growth. Columnar growth improves PV device properties as active layers.
- The EDS study revealed that the P1 and P2 thin films possessed near perfect Cu_2O stoichiometry and Cu_2O_3 stoichiometry, respectively.

- The Cu_2O thin films as active layers in PV cells should have a non-cracked and faultless surface because defects limit propagation to the absorber layer and transport of electrode carriers.
- The Cu_2O thin films as active layers should have minimal optical transmittance and maximal absorption to obtain a device with high-efficiency photoconversion.
- The P1 sample was determined to be optimal for PV devices. In the region from 800 to 1000 nm, the P1 sample had low optical transparency (up to 20%), whereas the P2 sample had up to 40% transparency. Hence, P2 thin films may not yield satisfactory results.
- The optical quality of the P1 and P2 films was relatively high, due to the low extinction coefficient values.
- The P1 and P2 samples were slightly shifted towards bulk copper (I) oxides – 2.0 eV. The anti-reflection structure plays an important role in the improvement of the PV [49]. The P1 sample exhibited better anti-reflective properties.
- This preliminary analysis of manufactured thin films revealed that the P1 sample was the most promising and future-oriented solution for PV application. The reason for the success was the smaller distance between the source and the substrate, and the higher value power of the modular platform deposition than for the P2 sample. A detailed analysis of the proposed solution is planned.

REFERENCES

[1] S. Korkmaz, B. Geçici, S.D. Korkmaz, R. Mohammadigharehbagh, S. Pat, S. Ozen, V. Senay, H.H. Yudar, Vacuum **131**, 142-146 (2016).

[2] N. Serin, T. Serin, Ş. Horzum, Y. Celik, Semicond. Sci. Technol. **20**, 398-401(2005).

[3] J. Morales, L. Sanchez, F. Martin, J. Ramos-Barrado, M. Sanchez, Thin Solid Films **474** (1-2), 133-140 (2005).

[4] A. Nalbant, Ö. Ertek, İ. Okur, Mater. Sci. Eng. B **178** (6), 368-374 (2013).

[5] H. Zhang, G. Zhao, L. Xu, Appl. Surf. Sci. **274**, 397-400, (2013).

[6] K. Mageshwari, R. Sathyamoorthy, Mater. Sci. Semicond. Process. **16**, 337-343, (2013).

[7] F. Chaffar Akkari, M. Kanzari, B. Rezig, Phys. J. Appl. Phys. **40**, 49-54 (2007).

[8] P. Markworth, X. Liu, J. Dai, W. Fan, T. Marks, R. Chang, J. Mater. Res. **16**, 2408-2414 (2001).

[9] A. Chen, H. Long, X. Li, Y. Li, G. Yang, P. Lu, Vacuum **83**, 927-930 (2009).

[10] S.C. Ray, Sol. Energy Mater. Sol. cells **68** (3-4), 307-312 (2001).

[11] X. Ma, G. Wang, K. Yukimura, M. Sun, Surf. Coat. Technol. **201** (15), 6712-6714, (2007).

[12] M. Yang, J.J. Zhu, J. Cryst. Growth **256** (1-2), 134-138 (2003).

[13] R. Kita, K. Kawaguchi, T. Hase, T. Koga, R. Itti, T. Morishita, J. Mater. Res. **9** 1280 (1994).

[14] P. Sawicka-Chudy, G. Wisz, Sz. Górny, Ł. Głowa, M. Sibiński, M. Cholewa, Journal of Nanoelectronics and Optoelectronics **13** (5), 715-721 (2018).

[15] H. Zhu, J. Zhang, C. Li, F. Pan, T. Wang, B. Huang, Thin Solid Films **517** (19), 5700-5704 (2009).

[16] M.H. Suhail, G. Mohan Rao, S. Mohan, Journal of Applied Physics **71**, 1421-1427 (1992).

[17] İ.Y. Erdoğan, Ö. Güllü, J. Alloys Compd. **492**, 378-383 (2010).

[18] D. Zappa, E. Comini, R. Zamani, J. Arbiol, J. Morante, G. Sberveglieri, Sens. Actuators B Chem. **182**, 7-15 (2013).

[19] D. Gopalakrishna, K. Vijayalakshmi, C. Ravidhas, Ceram. Int. **39**, 7685-7691 (2013).

[20] K. Kamimura, H. Sano, K. Abe, R. Hayashibe, T. Yamakami, M. Nakao, Y. Onuma, IEICE Trans. Electron. **E87-C** (2), 193-196 (2004).

[21] A.S. Reddy, G. Venkata, R.S. Uthanna, P. Sreedhara Reddy, Materials Letters **60** (13-14), 1617-1621 (2006).

[22] A.S. Reddy, S. Uthanna, P. Sreedhara Reddy, Applied Surface Science **253** (12), 5287-5292 2007.

[23] S.A. Reddy, S. Reddy Pamanji, S. Uthanna, UDC Magnetron Sputtered Pure and Al Doped Cu_2O Thin Films For Optoelectronic Devices, LAP Lambert Academic Publishing (2015).

[24] A.E. Rakhshani, Solid-State Electronics **29** (1), 7-17 (1986).

[25] Le Zhu Development of Metal Oxide Solar Cells through Numerical Modelling, PhD thesis.

[26] P. Sawicka-Chudy, M. Sibiński, G. Wisz, E. Rybak-Wilusz, M. Cholewa, Journal of Physics: Conference Series 1033, conference 1.

[27] T. Minami, Y. Nishi, T. Miyata, J. Nomoto, Applied Physics Express **4** (6), 062301-3 (2011).

[28] L.C. Olsen, F.W. Addis, W. Miller, Sol. Cells **7**, 247-279 (1982).

[29] A. Mittiga, E. Salza, F. Sarto, M. Tucci R. Applied Physics Letters **88** (16), 88-89 (2006).

[30] K. Akimoto, S. Ishizuka, M. Yanagita, Y. Nawa, Goutam K. Paul, T. Sakurai, Solar Energy **80** (6), 715-722 (2006).

[31] S. Hussain, C. Cao, Z. Usman, Z. Chen, G. Nabi, W.S. Khan, Z. Ali, F.K. Butt, T. Mahmood, Thin Solid Films **522**, 430-434 (2012)

[32] D. Li, C. Chien, S. Deora, P. Chang, E. Moulin, J. Lu, Chemical Physics Letters **501**, 446-450 (2011).

[33] A.R. Zainun, T. Sakamoto, U.M. Noor, M. Rusop, M. Ichimura, Materials Letters **66**, 254-256 (2012).

[34] M. Rokhmat, E. Wibowo, Sutisna, Khairurrijal, M. Abdullah, Procedia Engineering **170**, 72-77 (2017).

[35] A. Karapetyan, A. Reymers, S. Giorgio, C. Fauquet, L. Sajti, S. Nitsche, M. Nersesyan, V. Gevorgyan, W. Marine, Journal of Luminescence **159**, 325-332 (2015).

[36] P. Sawicka-Chudy, M. Sibiński, G. Wisz, E. Rybak-Wilusz, M. Cholewa, Official Proceedings MICROTHERM 2017, 71-72 (2017).

[37] P. Sawicka-Chudy, G. Wisz, Ł. Głowa, M. Sibiński, M. Cholewa, P. Potera, S. Adamiak E. Rybak-Wilusz, B. Cieniek, Journal of Nanoelectronics and Optoelectronics **13**, 995-1000 (2018).

[38] https://www.dcode.fr/image-histogram, accessed January 7th 2018.

[39] G. Wang, T. Jiu, P. Li, J. Li, C. Sun, F. Lua, J. Fang, Organic Electronics **15** (1), 29-34 (2014).

[40] D.E. Mencer, M.A. Hossain, R. Schennach, T. Grady, H. McWhinney, J.A.G. Gomes, M. Kesmez, J.R. Parga, T.L. Barr, D.L. Cocke, Vacuum **77** (1), 27-35 (2004).

[41] L.J. Meng, M.P. dos Santos, Thin Solid Films **250** (1-2), 26-32 (1994).

[42] J. Zheng, S. Bao, Y. Guo, P. Jin, Surface & Coatings Technology 240, 293-300 (2014)

[43] C. Malerba, F. Biccaria, C. Leonor, A. Ricardo, M. D'Incau, P. Scardi, A. Mittiga, Solar Energy Materials and Solar Cells **95** (10), 2848-2854 (2011).

[44] T. Ito, T. Kawashima, H. Yamaguchi, T. Masumi, S. Adachi, J. Phys. Soc. Jpn. **67**, 2125-2131 (1998).

[45] L.J. Meng, M.P. dos santos, Thin Solid Films **226** (1), 22-29 (1993).

[46] S. Wahyuningsih, G. Fadillah, R. Hidayat, A. Handono Ramelan, Procedia Chemistry **19**, 632-637 (2016).

[46] B.D. Viezbicke, S. Patel, B.E. Davis, D. P. Phys. Status Solidi B **252** (8), 1700-1710 (2015).

[47] F.K. Mugwang'a, P.K. Karimi, W.K. Njoroge, O. Omayio, S.M. Int. J. Thin Film Sci. Tec. **2** (1), 15-24 (2013).

[48] S. Wahyuningsih, G. Fadillah, R. Hidayat, A. Handono Ramelan, Procedia Chemistry **19**, 632-637 (2016).

[49] Z. Starowicz, M. Lipiński, R. P. Socha, K. Berent, G. Kulesza, P. Ozga, Journal of Sol-Gel Science and Technology (73), 563-571 (2015).